Iron under Earth's core conditions: Liquid-state thermodynamics and high-pressure melting curve from *ab initio* calculations

D. Alfè[1,2], G. D. Price[1] and M. J. Gillan[2]

[1]Research School of Geological and Geophysical Sciences
Birkbeck and University College London
Gower Street, London WC1E 6BT, UK

[2]Physics and Astronomy Department, University College London
Gower Street, London WC1E 6BT, UK

Ab initio techniques based on density functional theory in the projector-augmented-wave implementation are used to calculate the free energy and a range of other thermodynamic properties of liquid iron at high pressures and temperatures relevant to the Earth's core. The *ab initio* free energy is obtained by using thermodynamic integration to calculate the change of free energy on going from a simple reference system to the *ab initio* system, with thermal averages computed by *ab initio* molecular dynamics simulation. The reference system consists of the inverse-power pair-potential model used in previous work. The liquid-state free energy is combined with the free energy of hexagonal close packed Fe calculated earlier using identical *ab initio* techniques to obtain the melting curve and volume and entropy of melting. Comparisons of the calculated melting properties with experimental measurement and with other recent *ab initio* predictions are presented. Experiment-theory comparisons are also presented for the pressures at which the solid and liquid Hugoniot curves cross the melting line, and the sound speed and Grüneisen parameter along the Hugoniot. Additional comparisons are made with a commonly used equation of state for high-pressure/high-temperature Fe based on experimental data.

I. INTRODUCTION

The last few years have seen important progress in calculating the thermodynamic properties of condensed matter using *ab initio* techniques based on density-functional theory (DFT) [1–4]. There has been particular attention to the thermodynamics of crystals, whose harmonic free energy can be obtained from phonon frequencies computed by standard DFT methods [5–11]. The *ab initio* treatment of liquid-state thermodynamics is also important, and thermodynamic integration has been shown to be an effective way of calculating the DFT free energy of liquids [1,3,4]. These developments have made it possible to treat phase equilibria, including melting properties, by completely *ab initio* methods. We report here DFT free-energy calculations on high-pressure/high-temperature liquid iron, which we combine with earlier results on the solid [11] to obtain the complete melting curve and the variation of the volume and entropy of melting along the curve. We also present results for some key thermodynamic properties of the liquid, which we compare with data from shock experiments and other sources. The general methods developed here may be useful for other problems involving phase equilibria under extreme conditions. A brief report of this work was presented earlier [12].

The properties of high-pressure/high-temperature Fe are of great scientific importance because the Earth's core consists mainly of Fe, with a minor fraction of light impurities [13–15]. The melting curve is particularly important, since it provides one of the very few ways of estimating the temperature at the boundary between the liquid outer core and the solid inner core [16]. Because of this, strenuous efforts have been made to measure the melting curve [17–23], but the extreme pressures and temperatures required ($p \sim 330$ GPa, $T \sim 6000$ K) make the experiments very demanding. *Ab initio* calculations therefore have a major role to play, and several independent attempts to obtain the melting curve using different *ab initio* strategies have been reported recently [12,25,26]. The rather unsatisfactory agreement between the predictions makes a full presentation of the technical methods all the more important.

The calculation of melting properties using *ab initio* free energies was pioneered by Sugino and Car [1] in their work on the melting of Si at ambient pressure. Related methods were subsequently used by de Wijs *et al.* [3] to study the melting of Al. In both cases, thermodynamic integration (see e.g. Ref. [27]) was used to obtain the *ab initio* free energy from the free energy of a simple reference system, and we follow the same strategy here. The other recent calculations [25,26] on the high-pressure melting of Fe employed *ab initio* methods in a different way. Free energies were not calculated, but instead an empirical parameterised form of the total-energy function was fitted to DFT total energies calculated for representative configurations of the solid and liquid. The empirical energy function was then used in molecular dynamics simulations of very large systems containing coexisting solid and liquid.

The detailed DFT techniques used in this work are identical to those used in our work on h.c.p. Fe [11]. In particular, we use the generalised gradient approximation (GGA) for exchange-correlation energy, in the form known as Perdew-Wang 1991 [28,29], which reproduces very accurately a wide range of experimental properties of solid iron, as noted in more detail elsewhere [30–33]. We also use the projector-augmented-wave (PAW) implementation of DFT [33–35], which is an all-electron technique similar to other standard implementations such as full-potential augmented plane waves (FLAPW) [36], as well as being closely related to the ultrasoft pseudopotential method [37]. We have used the VASP code [38,39], which is exceptionally stable an efficient for metals, with the implementation of an extrapolation of the charge density which increases the efficiency of molecular dynamics simulations by almost a factor of two [40].

The calculation of melting properties demands very high precision for the free energies of the two phases, as emphasised elsewhere [3,11]. The required precision is set by the value of the entropy of melting, and one finds that in order to calculate the melting temperature to within 100 K the non-cancelling error in the free energies must be reduced to ~ 10 meV/atom. The use of identical electronic-structure methods in the two phases is clearly necessary; but it is certainly not sufficient, since the detailed free-energy techniques differ in the two phases. In the solid, we relied heavily on harmonic calculations, whereas the liquid-state calculations rely on relating the free energy to that of a reference liquid. It is therefore essential to reduce the statistical-mechanical errors below the tolerance, and we aim to demonstrate that this has been achieved.

In the next Section, we summarise the technical methods, and Sec. 3 then reports our results for the DFT free energy of liquid Fe over a wide range of thermodynamic states. Sec. 4 presents our calculated melting properties, which we compare with experimental results and the predictions of other *ab initio* calculations. Our free-energy results have been used to compute a variety of other thermodynamic quantities for the liquid, and we compare these in Secs. V and VI with direct shock measurements as well as published extrapolations of other experimental data. In the final Section, we give further discussion and a summary of our conclusions.

II. TECHNIQUES

The key thermodynamic quantity calculated in this work is the *ab initio* Helmholtz free energy F, which, with the statistical mechanics of the nuclei treated in the classical limit, is:

$$F = -k_{\rm B}T \ln \left\{ \frac{1}{N! \Lambda^{3N}} \int d\mathbf{R}_1 \ldots d\mathbf{R}_N \, \exp \left[-\beta U_{\rm AI}(\mathbf{R}_1, \ldots \mathbf{R}_N; T_{\rm el}) \right] \right\} \;, \tag{1}$$

where $\mathbf{R}_i$ $(i = 1, \ldots N)$ are the positions of the N nuclei, $\Lambda = h/(2\pi M k_{\rm B}T)^{1/2}$ is the thermal wavelength, with M the nuclear mass and $\beta = 1/k_{\rm B}T$. The quantity $U_{\rm AI}(\mathbf{R}_1, \ldots \mathbf{R}_N; T_{\rm el})$ is the DFT electronic free energy calculated with the N nuclei fixed at positions $\mathbf{R}_1, \ldots \mathbf{R}_N$. This is given, following the Mermin formulation of finite-temperature DFT [41], by $U_{\rm AI} = E - TS$, where the DFT energy E is the usual sum of kinetic, electron-nucleus, Hartree and exchange-correlation terms, and S is the electronic entropy, given by the independent-electron formula: $S = -k_{\rm B}T_{\rm el} \sum_i [f_i \ln f_i + (1 - f_i) \ln(1 - f_i)]$, with f_i the thermal (Fermi-Dirac) occupation number of orbital i. In exact DFT, the exchange correlation (free) energy $E_{\rm xc}$ has an explicit dependence on $T_{\rm el}$ but we assume here that $E_{\rm exc}$ has its zero-temperature form. It was shown in Ref. [11] that quantum corrections to the classical approximation to the free energy are negligible in the high-temperature solid, and the same will be true *a fortiori* in the liquid.

Our earlier work [33] should be consulted for technical details of the PAW implementation of DFT that we use. We note here that under Earth's core conditions it is not accurate enough to neglect the response of the $3p$ electrons, and in principle these should be explicitly included in the valence set along with the $3d$ and the $4s$ electrons. However, as shown earlier [32,33], the computational effort of including $3p$ electrons explicitly can be avoided with almost no loss of precision by mimicking the effect of the $3p$ electrons by an effective pair potential. The procedure for constructing this pair potential was described in Ref. [33]. The pair potential used here is exactly the same as we used in our thermodynamic calculations on the h.c.p. solid, so that a good cancellation of any residual errors is expected. To avoid any possible doubt on this score, we have also done spot checks on the effect of including both $3s$ and $3p$ electrons explicitly in the valence set, as reported in Sec. IV. The outermost core radius in our PAW calculations is 1.16 Å. At Earth's core pressures, the atoms in both liquid and solid come closer than the diameter of the ionic cores, which therefore overlap. We will show in Sec. IV that this too has only a very small effect on the free energies.

The present calculations, like those reported earlier on the h.c.p. solid, make use of 'thermodynamic integration' [27], which is a completely general technique for determining the difference of free energies $F_1 - F_0$ of two systems whose total-energy functions are U_1 and U_0. The basic idea is that $F_1 - F_0$ represents the reversible work done on continuously and isothermally switching the energy function from U_0 to U_1. To do this switching, a continuously variable energy function U_λ is defined as:

$$U_\lambda = (1 - \lambda)U_0 + \lambda U_1 \,, \tag{2}$$

so that the energy goes from U_0 to U_1 as λ goes from 0 to 1. In classical statistical mechanics, the work done in an infinitesimal change $d\lambda$ is:

$$dF = \langle dU_\lambda/d\lambda \rangle_\lambda d\lambda = \langle U_1 - U_0 \rangle_\lambda d\lambda \,, \tag{3}$$

where $\langle \cdot \rangle_\lambda$ represents the thermal average evaluated for the system governed by U_λ. It follows that:

$$F_1 - F_0 = \int_0^1 d\lambda \, \langle U_1 - U_0 \rangle_\lambda \,. \tag{4}$$

We use this technique to calculate the *ab initio* free energy F_{AI} of liquid Fe by identifying U_1 as the *ab initio* total energy function $U_{\mathrm{AI}}(\mathbf{R}_1, \ldots \mathbf{R}_N)$ and U_0 as the total energy $U_{\mathrm{ref}}(\mathbf{R}_1, \ldots \mathbf{R}_N)$ of a simple model reference system, whose free energy F_{ref} can be calculated. Then F_{AI} is given by:

$$F_{\mathrm{AI}} = F_{\mathrm{ref}} + \int_0^1 d\lambda \, \langle U_{\mathrm{AI}} - U_{\mathrm{ref}} \rangle_\lambda \,. \tag{5}$$

In practice, we calculate $\langle U_{\mathrm{AI}} - U_{\mathrm{ref}} \rangle_\lambda$ for a suitable set of λ values, and perform the integration numerically. The average $\langle U_{\mathrm{AI}} - U_{\mathrm{ref}} \rangle_\lambda$ is evaluated at each λ using constant-temperature *ab initio* molecular dynamics, with the time evolution generated by the total-energy function $U_\lambda = (1 - \lambda)U_{\mathrm{ref}} + \lambda U_{\mathrm{AI}}$.

As explained in more detail elsewhere [11], the computational effort needed to perform the thermodynamic integration is greatly reduced if the fluctuations of the energy difference $\Delta U \equiv U_{\mathrm{AI}} - U_{\mathrm{ref}}$ are small, for two reasons. First, the amount of sampling needed to calculated $\langle \Delta U \rangle_\lambda$ to a given precision is reduced; second, the variation of $\langle \Delta U \rangle_\lambda$ as λ goes from 0 to 1 is reduced. In fact, if the fluctuations $\delta \Delta U \equiv \Delta U - \langle \Delta U \rangle_{\mathrm{AI}}$ are small enough, one can neglect this variation and approximate $F_{\mathrm{AI}} \simeq F_{\mathrm{ref}} + \langle \Delta U \rangle_{\mathrm{AI}}$, with the average taken in the *ab-initio* ensemble. If this is not good enough, the next approximation is readily shown to be:

$$F_{\mathrm{AI}} \simeq F_{\mathrm{ref}} + \langle \Delta U \rangle_{\mathrm{AI}} + \frac{1}{2 k_{\mathrm{B}} T} \langle (\delta \Delta U)^2 \rangle_{\mathrm{AI}} \,. \tag{6}$$

Our task is therefore to search for a model U_{ref} for which the fluctuations $U_{\mathrm{AI}} - U_{\mathrm{ref}}$ are as small as possible.

The problem of mimicking the fluctuations of *ab initio* energy U_{AI} in high-p/high-T liquid Fe using a reference system was studied in detail in a recent paper [33]. We showed there that a U_{ref} consisting of a sum of pair potentials:

$$U_{\mathrm{ref}} = U_{\mathrm{th}} + U_{\mathrm{pair}} \,, \tag{7}$$

in which

$$U_{\mathrm{pair}} = \frac{1}{2} \sum_{i \neq j} \phi(|\, \mathbf{R}_i - \mathbf{R}_j \,|) \,, \tag{8}$$

can be arranged to mimic the fluctuations of U_{AI} very precisely, if we choose $\phi(r)$ to be a repulsive inverse-power potential $\phi(r) = B/r^\alpha$, with suitable values of B and α. In this expression for U_{ref}, we have included a term U_{th} which depends on thermodynamic state, but does not depend on the positions $\mathbf{R}_i$. We define this U_{th} so as to minimize the mean square value of ΔU, which requires the following condition:

$$\langle \Delta U \rangle_{\mathrm{AI}} \equiv \langle U_{\mathrm{AI}} - U_{\mathrm{pair}} - U_{\mathrm{th}} \rangle_{\mathrm{AI}} = 0 \,. \tag{9}$$

It might at first seem surprising that such a simple U_{ref} can reproduce U_{AI} accurately, since it does not explicitly represent the metallic bonding due to partial filling of the $3d$-band, which is absorbed into the term U_{th}. However, the only requirement on U_{ref} is that the fluctuations $\delta \Delta U$ should be small for the given liquid state, and we shall demonstrate below that this is indeed achieved. We comment further on this question in Sec. VII.

The free energy of the reference system can be expressed as:

$$F_{\mathrm{ref}} = U_{\mathrm{th}} + F_{\mathrm{pair}} \,, \tag{10}$$

where F_{pair} is the free energy associated with U_{pair}. An important advantage of our chosen form of U_{ref} is that F_{pair} depends non-trivially only on a single thermodynamic variable, rather than depending separately on temperature T and atomic number density n. Let $F_{\mathrm{pair}}^x \equiv F_{\mathrm{pair}} - F_{\mathrm{pg}}$ be the excess free energy of the reference system, *i.e.*

3

the difference between F_{pair} and the free energy F_{pg} of the perfect gas at the given T and n. Then the quantity $f_{\text{pair}}^x \equiv F_{\text{pair}}^x/Nk_BT$ depends only on the dimensionless thermodynamic parameter ζ defined as:

$$\zeta = Bn^{\alpha/3}/k_BT \ . \tag{11}$$

This simplifies the representation of F_{ref}, since we can write:

$$F_{\text{ref}} = U_{\text{th}} + F_{\text{pg}} + Nk_BT f_{\text{pair}}^x(\zeta) \ . \tag{12}$$

We also expect the representation of U_{th} to be simple. Note first that since U_{th} is defined so that $\langle \Delta U \rangle_{\text{AI}} = 0$, then from Eqn (9) we must have:

$$U_{\text{th}} = \langle U_{\text{AI}} - U_{\text{pair}} \rangle_{\text{AI}} \ . \tag{13}$$

Now if the fluctuations of $U_{\text{AI}} - U_{\text{pair}}$ are indeed small, then the value of $\langle U_{\text{AI}} - U_{\text{pair}} \rangle_{\text{AI}}$ should be very close to the value of $U_{\text{AI}} - U_{\text{pair}}$ evaluated at zero temperature with all atoms on the sites of the perfect h.c.p. lattice having the same density as the liquid. Denoting by U_{AI}^0 and U_{pair}^0 the values of the zero-temperature *ab initio* and pair-potential energies for the perfect lattice, and defining $U_{\text{th}}^0 \equiv U_{\text{AI}}^0 - U_{\text{pair}}^0$, we can then write:

$$U_{\text{th}} = U_{\text{th}}^0 + \delta U_{\text{th}} \ , \tag{14}$$

where δU_{th} will be a small quantity depending weakly on volume and temperature. The accurate computation and representation of U_{AI}^0 were discussed in Ref. [11], and the accurate computation of U_{pair}^0 is clearly trivial, so that the treatment of U_{th}^0 is straightforward. The small difference $\delta U_{\text{th}} \equiv \langle U_{\text{AI}} - U_{\text{pair}} \rangle_{\text{AI}} - U_{\text{th}}^0$ is evaluated from the AIMD simulations described in Sec. III C.

We conclude this Section by summarising our route to the calculation of the *ab initio* free energy F_{AI} of the liquid. We employ Eqn (6), ignoring the higher-order fluctuation terms. Recalling that $\langle \Delta U \rangle_{\text{AI}} = 0$, and combining Eqns (12) and (14), we have:

$$\begin{aligned} F_{\text{AI}} &\simeq F_{\text{ref}} + \langle (\delta \Delta U)^2 \rangle_{\text{AI}}/2k_BT \\ &= U_{\text{th}}^0 + \delta U_{\text{th}} + F_{\text{pg}} + Nk_BT f_{\text{pair}}^x(\zeta) + \langle (\delta \Delta U)^2 \rangle_{\text{AI}}/2k_BT \ . \end{aligned} \tag{15}$$

We now turn to the calculation of the reduced free energy $f_{\text{pair}}^x(\zeta)$ of the reference system and the small quantities δU_{th} and $\langle (\delta \Delta U)^2 \rangle_{\text{AI}}$. We shall also give evidence that with our chosen reference model the higher-order fluctuation terms omitted from Eqn (15) are indeed negligible.

III. FREE ENERGY OF THE LIQUID

A. Inverse-power reference system

The PAW calculations used to validate the inverse-power reference system are those reported in Ref. [33]. They consist of a set of AIMD simulations performed at 16 thermodynamic states covering the temperature range $3000 - 8000$ K and the pressure range $60 - 390$ GPa. All the simulations were performed on a 67-atom system using Γ-point sampling, with a time step of 1 fs. We stress that such a small system with such limited sampling cannot be expected to yield very precise results for thermodynamic quantities, and our only purpose here is to demonstrate the adequacy of the reference system. At each thermodynamic state, the system was equilibrated using the reference system itself, and AIMD data were then accumulated for a time span of 5 ps.

We showed in Ref. [33] that the inverse-power model, with parameters $\alpha = 5.86$ and B chosen so that for $r = 2$ Å the potential $\phi(r)$ is 1.95 eV, reproduces very closely the *ab initio* liquid for the state $T = 4300$ K, $\rho = 10700$ kg m^{-3}. We have studied the strength of the $\delta \Delta U$ fluctuations for all 16 thermodynamic states, using exactly the same reference model for all states, and we report in Table I the normalized strength of these fluctuations, which we characterize by the quantity $\sigma \equiv \left[\langle (\delta \Delta U)^2 \rangle_{\text{AI}}/N \right]^{1/2}$. Two points should be noted: First, σ is small, since its typical value of 100 meV is markedly smaller than the typical thermal energies k_BT (258 meV at the lowest temperature of 3000 K). Once σ is as small as this, little is gained by further improvement of the reference system. Second, σ does not vary strongly with thermodynamic state, so that the reference system specified by the values of α and B given above can be used for all the thermodynamic states of interest here.

B. Free energy of reference system

In order to cover the range of thermodynamic states of liquid Fe that interests us, we need accurate values of the excess free energy of the reference system for ζ values going from 2.5 to 5.0. There have been many studies of the thermodynamic properties of inverse-power systems, including one on the free energy of the liquid $1/r^6$ system [42], but since these do not provide what we need we have made our own calculations of $f_{\mathrm{ref}}^x(\zeta)$ for the $1/r^{5.86}$ case. Our strategy is to start with standard literature values for the excess free energy of the Lennard-Jones (LJ) liquid (we use the results reported in Ref. [43]), and to use thermodynamic integration to go from the LJ system to the inverse-power system, so that U_0 and U_1 in Eqns (2–3) represent the LJ and inverse-power total energies respectively. In doing this, our target was to keep technical errors small enough so that the final free energy F_{ref} is correct to better than 5 meV/atom.

We note the following technical points. The calculations were done at a standard volume per atom, usually taken to be 8.67 Å^3, with the temperature chosen to give the required value of ζ. Ewald techniques were used to avoid cutting off the inverse-power potential at any distance – we regarded this as essential, since a cut-off would compromise the scaling properties of the reference system. The classical molecular dynamics simulations used to compute $\langle U_1 - U_0 \rangle_\lambda$ were done using the constant-temperature technique, with each atom taken to have a mass of 55.86 a.u., and the time-step set equal to 1 fs. For each thermodynamic state, we are free to choose any convenient values for the LJ parameters ϵ and σ. Our criterion for choosing these is that the fluctuations of $U_1 - U_0$ should be kept reasonably small, but with the proviso that the initial LJ system must be in the liquid state. In many cases, we have checked for consistency by using different ϵ and σ values. Since we require $f_{\mathrm{ref}}^x(\zeta)$ in the thermodynamic limit of infinite system size, we have made careful checks on size effects. Tests on systems containing up to 499 atoms show that size errors in $f_{\mathrm{ref}}^x(\zeta)$ are less than 1 meV/atom, and this is small enough to ensure that F_{ref} has a precision of better than 5 meV. Most of this error arises from the error in the literature values of the LJ free energy. As a further check on our techniques, we have done calculations on the $1/r^6$ system at selected thermodynamic states, and compared with the free energy results of Laird and Haymet [42].

We have checked our procedures by repeating most of the calculations using the perfect gas as reference system, so as to be free from possible errors in the free energy of the LJ system. For these calculations we used a different form for U_λ, namely

$$U_\lambda = (1 - \lambda^2)U_0 + \lambda^2 U_1 \;, \tag{16}$$

where U_1 is the total energy of the inverse power system and $U_0 = 0$ is that of the perfect gas. Using this functional form Eq. (4) becomes

$$F_1 - F_0 = \int_0^1 d\lambda \, 2\lambda \langle U_1 - U_0 \rangle_\lambda \;. \tag{17}$$

The advantage of using this different functional form for U_λ is that the value of the integrand does not need to be computed for $\lambda = 0$, where the dynamics of the system is that of the perfect gas. In this case, since there are no forces in the system, there is nothing to prevent the atoms from overlapping, and the potential energy U_1 diverges. Not computing the integrand at $\lambda = 0$ only partially solves this problem, since for small values of λ the forces on the atoms are small, the atoms can come close together, and the potential energy U_1 fluctuates violently. However, we found that by performing long enough simulations, typically 1 ns, we could calculate the integral with an accuracy of *ca.* 1 meV/atom. These calculations with the perfect-gas reference system give excess free energies of the inverse power system that are systematically 5 meV/atom lower than those obtained using the LJ reference system. Our belief is that the discrepancy arises from a small systematic error in the free energies given in Ref. [43].

After all these tests, calculations of $f_{\mathrm{ref}}^x(\zeta)$ were done at a regularly spaced set of ζ values at intervals of 0.25, and we found that the results could be fitted to the required precision by the following 3rd-degree polynomial:

$$f_{\mathrm{ref}}^x(\zeta) = \sum_{i=0}^3 c_i \zeta^i \;. \tag{18}$$

The values of the coefficients are: $c_0 = 1.981, c_1 = 5.097, c_2 = 0.1626, c_3 = 0.009733$.

C. From reference to full *ab initio*

To achieve our target precision of 10 meV/atom in the *ab initio* free energy F_{AI} of the liquid, two sources of error must be studied: system size effects and electronic k-point sampling. An important point to note is that these errors

only affect the small terms δU_{th} and $\langle (\delta \Delta U)^2 \rangle_{\text{AI}}/2k_{\text{B}}T$ in Eqn (15), since $f_{\text{ref}}^x(\zeta)$ refers already to the infinite system, and k-point errors in U_{th}^0 are negligible. We also study the validity of neglecting the higher-order fluctuation terms in Eqn (15).

We focus first on the quantity δU_{th} in Eqn (15). To study size errors in this quantity, we calculated the thermal average $\langle U_{\text{AI}} - U_{\text{pair}} \rangle_{\text{AI}}$ for a range of system sizes. These test calculations were done on systems of up to 241 atoms at $V = 8.67$ Å^3/atom and $T = 4300$ K using Γ-point sampling. The preparation and equilibration of these systems were done using the inverse-power reference system. Since the latter so closely mimics the *ab initio* system for the 67-atom cell, it should provide a well equilibrated starting point for *ab initio* simulation of larger systems. The duration of all the *ab initio* simulations after equilibration was 1 ps. The results of these tests are summarised in Table II, where we report the value of δU_{th} per atom, i.e. the quantity $\delta U_{\text{th}}/N \equiv [\langle U_{\text{AI}} - U_{\text{pair}} \rangle_{\text{AI}} - U_{\text{th}}^0]/N$ (see Sec. II). Since U_{th}^0/N is independent of the system size, the variation of the reported quantity arises solely from size dependence of $\langle U_{\text{AI}} - U_{\text{pair}} \rangle_{\text{AI}}/N$. We see that with ~ 125 atoms $\delta U_{\text{th}}/N$ is converged to better than 5 meV/atom, and that already with 67 atoms the size error is of the order of 10 meV/atom.

We tested for k-point errors in δU_{th} by performing calculations using both four and 32 Monkhorst-Pack [44] sampling points. Since explicit AIMD calculations with so many k-points would be extremely expensive, we use the following procedure. From an existing Γ-point simulation we take a set of typically 10 atomic configurations separated by 0.1 ps. The *ab initio* total energies of these configurations calculated with the different k-point samplings are then compared. For sampling with four k-points, we did calculations on systems of up to 241 atoms, but the heavier calculations with 32 k-points were done only on the 67-atom system. The results of these tests for the thermodynamic state $V = 8.67$ Å^3/atom and $T = 4300$ K are also reported in table II, where we see that for the smallest system containing 67 atoms the difference with respect to a calculation with the Γ-point only is ~ 9 meV/atom, but as the number of atoms in the cell is increased above ~ 125 the difference becomes negligible. The result for the calculation with 32 k-points is identical to the one with four k-points and is not reported in the table. We also found that fluctuations of the energy differences between the calculations done with the Γ-point only and those with 4 k-points are extremely small.

Similar, but less extensive, tests of system-size and k-point errors have also been performed at the state $V = 6.97$ Å^3/atom, $T = 6000$ K, and we find that the variation of these errors with system size is numerically almost the same as before. The indication is therefore that δU_{th} can be obtained to a precision of *ca.* 5 meV/atom from simulations on systems of 125 atoms or more. Unfortunately, it is not practicable yet to do all our AIMD simulations with this system size, and in practice we have computed δU_{th} from Γ-point simulations on the 67-atom system, and corrected the results by adding 10 meV/atom, which from the present evidence appears to the almost constant error in the Γ-point 67-atom results.

As expected, the numerical values of δU_{th} are small, and depend weakly on temperature and pressure across the range of thermodynamic states of interest. We find that they can be represented to within ~ 3 meV/atom by a sum of third-degree polynomials in V and T:

$$\delta U_{\text{th}}/N = \sum_{i=0}^{3} \left(a_i V^i + b_i T^i \right) \ , \tag{19}$$

with the following fitting parameters (units of eV, Å and K): $a_0 = 0.649$; $a_1 = -4.33 \times 10^{-2}$; $a_2 = -4.19 \times 10^{-3}$; $a_3 = 6.48 \times 10^{-5}$; $b_0 = 0.296$; $b_1 = -6.51 \times 10^{-5}$; $b_2 = 7.46 \times 10^{-9}$; $b_3 = -2.07 \times 10^{-13}$.

To test the validity of neglecting the higher-order fluctuation terms omitted from Eqn (15), we have performed full thermodynamic integration for four different thermodynamic states, the first three with $V = 8.67$ Å^3/atom and $T = 4300, 6000$ and 8000 K and the fourth with $V = 6.97$ Å^3/atom and $T = 8000$ K, using the five equally spaced λ values 0, 0.25, 0.5, 0.75 and 1.0. These calculations were done using Γ-point sampling on the system of 67 atoms. We have seen that this system size is not big enough to yield the required precision for F_{AI}, but it should certainly be enough to test the adequacy of the second-order formula. In Table III we report a comparison between the results obtained from the integral using the five λ values and those from the second order formula, and we see that they are practically indistinguishable. The Table also indicates that the term $\langle (\delta \Delta U)^2 \rangle_{\text{AI}}/2k_{\text{B}}T$ is rather insensitive to thermodynamic state and can be approximated to the required precision by setting it equal to 10 meV/atom. We have used this constant value in evaluating the *ab initio* free energy by Eqn (15).

IV. MELTING PROPERTIES

From our parameterized formulas for the *ab initio* Helmholtz free energies $F(V, T)$ of the h.c.p. solid (Ref. [11]) and the liquid (present work), we immediately obtain the Gibbs free energies $G(p, T) \equiv F(V, T) + pV$, and for each

pressure the melting temperature T_m is determined as the T at which the latter free energies are equal for the solid and liquid. The resulting melting curve is reported in Fig. 1 for pressures from 50 to 350 GPa. On the same plot, we show the *ab initio* melting curve reported very recently by Laio *et al.* [25]. We also compare with experimental melting curves or points obtained by shock experiments or by static-compression using the diamond anvil cell (DAC). DAC determinations of the melting curve of Fe and other transition metals have been performed by several research groups [17–20]. The early results of Williams *et al.* [21] lie considerably above those of other groups, and are now generally discounted. This still leaves a range of *ca.* 400 K in the experimental T_m at 100 GPa. Even allowing for this uncertainty, we acknowledge that our melting curve lies appreciably above the surviving DAC curves, with our T_m being above that of Shen *et al.* [19] by *ca.* 400 K at 100 GPa. We return to this discrepancy below.

Shock measurements should in principle be able to fix a point on the high-pressure melting curve at the thermodynamic state where melting first occurs on the Hugoniot. However, temperature is notoriously difficult to measure in shock experiments. The temperatures obtained by Yoo *et al.* [22] using pyrometric techniques are generally regarded as being too high by at least 1000 K. This has been confirmed by our recent *ab initio* calculations [11] of Hugoniot temperature for h.c.p. Fe. We therefore disregard their data point on the melting curve. In the shock measurements of Brown and McQueen [23] and Nguyen and Holmes [24], no attempt was made to measure temperature, which was estimated using models for the specific heat and Grüneisen parameter; the approximate validity of these models is supported by our *ab initio* calculations [11] on h.c.p. Fe. However, the identification of the Hugoniot melting point has been hampered by the possible existence of a solid-solid transition. In their measurements of sound velocity on the Hugoniot, Brown and McQueen [23] believed that they had observed a solid-solid transition as well as a separate melting transition. The new shock results of Nguyen and Holmes [24] using improved techniques indicate that there is no solid-solid transition, and we place greater weight on their Hugoniot melting point. We plot in Fig. 1 the point reported by Brown and McQueen [23] as lying on the melting curve, though for the reasons just explained, we are cautious about accepting it. We also plot the point obtained from the measurements of Nguyen and Holmes [24]. The pressure of 221 GPa is taken directly from their measurement of the onset of melting, while the temperature at this point is taken from our calculation of the Hugoniot temperature of the h.c.p. solid at this pressure, as reported in Ref. [11] (see also following section).

We now consider possible sources of error in our DFT calculations. First, we recall that even with the best available GGA for exchange-correlation energy the low-temperature $p(V)$ relation for h.c.p. Fe is not in perfect agreement with experiment. This has been shown by a number of independent calculations using all-electron techniques [30,31] as well as pseudopotential [32] and PAW [33,35] techniques, all of which agree closely with each other. Roughly speaking, the pressure is underpredicted by *ca.* 10 GPa at near-ambient pressures and by *ca.* 8 GPa in the region of 300 GPa. The pressure error can be thought of as arising from an error in the Helmholtz free energy, so that the true free energy F_{true} can be written as $F_{\text{true}} = F_{\text{GGA}} + \delta F$, where F_{GGA} is our calculated free energy and δF is the correction. If we take the pressure error $\delta p \equiv -(\partial \delta F/\partial V)_T$ to be linear in the volume, then δF can be represented as $\delta F = b_1 V + b_2 V^2$, where b_1 and b_2 are adjustable parameters determined by least-squares fitting to the experimental pressure. If we now neglect the temperature dependence of δF, and simply add $\delta F(V)$ to the calculated free energies of solid and liquid, this gives a way of gauging our likely errors. We find that this free-energy correction leads to a lowering of the melting curve by *ca.* 350 K in the region of 50 GPa and by *ca.* 70 K in the region of 300 GPa.

The second error source we consider is the PAW implementation, and specifically our choice of the division into core and valence states, and the PAW core radii. As mentioned earlier, at Earth's core pressures the $3p$ electrons, and to a lesser extent the $3s$ electrons, must be treated as valence states. Moreover, the choice of the maximum PAW core radius may also affect the calculations, because under such high pressures and temperatures the atoms come so close that the cores overlap. These errors may affect the melting curve if they fail to cancel between the liquid and the solid. To check both these possible problems, we have performed trial PAW calculations with the much smaller core radius of 0.85 Å and with both $3s$ and $3p$ states in the valence set; with this choice of core radius the overlap of the cores in the liquid and the high temperature solid is almost negligible. We have then used Eq. (6) to calculate the free energy difference between the systems described with the two PAW approximations, repeating the calculations for both the liquid and the solid. To do that we have drawn two sets of 30 statistically independent configurations from two long simulations performed with the original PAW approximation on the solid and the liquid at $V = 7.18$ Å^3/atom and $T = 6700$ K. As expected, we find a significant shift in the total electronic (free) energies. This shift is almost constant, thus validating the use of Eq. (6), but the important result is that it is almost the same for the liquid and the solid, the two numbers being $F_{\text{hard}}^l - F_{\text{soft}}^l = -0.210$ eV/atom $F_{\text{hard}}^s - F_{\text{soft}}^s = -0.204$ eV/atom. Here, F_{hard}^l is the free energy calculated with small core and $3s$ and $3p$ states in valence, and F_{soft}^l the free energy with large core and the $3s$ and $3p$ frozen in the core, plus the effective pair-potential; the superscripts s and l indicate the solid and the liquid respectively. The effect is small, and stabilises the liquid by 6 meV/atom, which has the effect of shifting the melting curve down by ~ 60 K.

As we show in Fig. 1, if we include both these corrections they bring our low-temperature melting curve into quite respectable agreement with the DAC measurements of Shen *et al.*, while leaving the agreement with the shock

points of Nguyen and Holmes essentially unaffected. There is still a considerable discrepancy with the DAC curve of Boehler [17] and the *ab initio* results of Laio *et al.* [25]

We now turn to the changes of volume and entropy on melting. Our calculated volume of melting (volume of liquid minus volume of coexisting h.c.p. solid at each pressure expressed as a percentage of the volume of the solid at that point) is plotted as a function of pressure in Fig. 2. We also show the melting volume predicted by the *ab initio* calculations of Laio *et al.* [25] at the pressure 330 GPa, and it is encouraging to note that their value of 1.6 % is quite close to ours. The free-energy correction discussed above makes only a small difference to the calculated volume of melting: at 50 GPa the correction makes the volume of melting increase from 5.0 to 5.8 %, while at 300 GPa it is affected by less than 0.1 %. The most striking feature of our results is the steep decrease of ΔV by a factor of about three in the range from 50 to 200 GPa, and its approximate constancy after that.

Our predicted entropy of melting ΔS_m (entropy per atom of liquid minus entropy per atom of coexisting solid) is plotted as a function of pressure in Fig. 3, where we also show the *ab initio* value of Laio *et al.* [25] at 330 GPa. The agreement of our value (1.05 k_B) with theirs (0.86 k_B) is reasonably close. The entropy of melting also decreases with increasing p, but more moderately than $\Delta V/V$, the decrease between 50 and 200 GPa being only 30 %. We note the relevance to the slope of the melting curve, given by the Clausius-Clapeyron relation: $dT_m/dp = \Delta V/\Delta S$. (This relation is satisfied identically by our results, since they are all derived from free energies.) The strong decrease of dT_m/dp between 50 and 200 GPa and its approximate constancy thereafter is mainly due to the variation of $\Delta V/V$.

V. HUGONIOT PROPERTIES

Since shock experiments are the only direct way of obtaining thermodynamic information for high-p/high-T liquid Fe, it is important to test our predictions against the available shock data. The data that emerge most directly from shock experiments consist of a relation between the pressure p_H and the molar volume V_H on the so-called Hugoniot line, which is the set of thermodynamic states given by the Rankine-Hugoniot formula [45]:

$$\frac{1}{2}p_H(V_0 - V_H) = E_H - E_0 \, , \tag{20}$$

where E_H is the molar internal energy behind the shock front, and E_0 and V_0 are the molar internal energy and volume in the zero-pressure state ahead of the front. The pressure-volume and temperature-pressure relations on the Hugoniot are straightforwardly obtained from our *ab initio* calculations: for a given V_H, one seeks the temperature T_H at which the Rankine-Hugoniot relation is satisfied, and from this one obtains p_H (and, if required, E_H). In experiments on Fe, V_0 and E_0 refer to the zero-pressure b.c.c. crystal. We obtain E_0 directly from GGA calculations that we performed on the ferromagnetic b.c.c. crystal, as described earlier [11], but we use the experimental value of V_0. The slight shift produced by using instead the theoretical value of V_0 was noted earlier [11]. Melting in shock experiments is usually detected by monitoring the sound velocity [22,23], which shows marked discontinuities of slope along the Hugoniot. In a simple melting transition, there are discontinuities at two characteristic pressures p_s and p_l, which are the points where the solid and liquid Hugoniots meet the melting curve. Below p_s, the material behind the shock front is entirely solid, while above p_l it is entirely liquid; between p_s and p_l, the material is a two-phase mixture.

We present in Fig. 4 our calculated $T_H(p_H)$ Hugoniot curve for the liquid, together with our curve for the solid reported earlier [11] and our *ab initio* melting curve. Without the free energy correction δF of Sec. IV, we find $p_s = 229$ and $p_l = 285$ GPa. The very recent shock data of Nguyen and Holmes [24] give values of 221 and 260 GPa respectively, so that our p_s value is very close to theirs, and our p_l value is also not very different.

If the correction δF is included in calculating the melting curve, then for consistency it must be included also in the solid and liquid Hugoniots. It is straightforward to obtain the corrected p_H and E_H as a function of V_H for the two phases. But in the Rankine-Hugoniot equation we also need E_0 for the b.c.c. crystal, and this will be subject to a correction similar to δF, but of unknown size. To supply the missing information, we add to the *ab initio* energy of b.c.c. Fe a correction term δF_{bcc}, which we represent as $c_1 + c_2 V$. The constants c_1 and c_2 are fixed by requiring that the equilibrium volume of the b.c.c. crystal and the low-temperature transition pressure between the b.c.c. and h.c.p. phases be correctly given. The resulting 'corrected' $T_H(p_H)$ Hugoniots of the solid and liquid are reported in Fig. 4. The shifts in the curves are of about the same size as those discussed earlier [11] for the solid when we replaced the calculated b.c.c. volume V_0 in the Rankine-Hugoniot equation by its experimental value, and are an indication of the inherent uncertainty due to DFT errors. The corrected values $p_s = 243$, $p_l = 298$ GPa are now in somewhat poorer agreement with the experimental values. This is a rather sensitive test of DFT errors, since the shallow angle at which the Hugoniot curves cross the melting line amplifies the effect of the errors.

We now turn to our liquid-state results for $p_H(V_H)$ compared with the shock data of Brown and McQueen [23] (Fig. 5), including for completeness our results for the solid reported earlier [11]. We report results both with and

without the free energy correction δF, using the experimental b.c.c. volume V_0 in the Rankine-Hugoniot equation in both cases. We mark on the Figure the volumes above which the shocked material is entirely solid and below which it is entirely liquid. Above the upper volume, we report our calculated h.c.p. Hugoniots, and below the lower volume the liquid Hugoniots. In the interval between them, we linearly mix the two. We note that the δF correction makes little difference to the liquid Hugoniot, which lies above the experimental values by *ca.* 3 %.

Shock experiments on Fe have given values for the adiabatic sound speed $v_S = (K_S/\rho)^{1/2}$ of the liquid, with K_S the adiabatic bulk modulus and ρ the mass density. Fig. 6 shows our *ab initio* values for v_S of the liquid as a function of pressure on the Hugoniot, both with and without the δF correction, compared with the shock data of Refs. [23]. Up to the pressure of ~ 260 GPa, the experimental points refer to the solid or the two-phase region, so it is in the liquid region above this pressure that the comparison is significant. In that region, our agreement with the experimental data is close, the discrepancies being ~ 2 and < 1 % for our uncorrected and corrected v_S values respectively.

We conclude this Section by reporting results for the Grüneisen parameter γ on the liquid Hugoniot. This parameter is defined as $\gamma \equiv V(\partial p/\partial E)_V = \alpha K_T V_\mathrm{m}/C_v$, with α the volume expansion coefficient, K_T the isothermal bulk modulus, C_v the constant-volume molar specific heat, and V_m the molar volume. Assumptions or estimates of its values have played a key role in constructing parameterised equations of state for Fe. Our calculated γ on the liquid Hugoniot is almost exactly constant, varying in the narrow range from 1.51 to 1.52 as p goes from 280 to 340 GPa.

VI. THERMODYNAMICS OF THE LIQUID

Although directly measured data on high-p/high-T liquid Fe all come from shock experiments, attempts have been made to combine these data with measurements at lower p and T using parameterised models for quantities such as K_S, γ and C_v to estimate thermodynamic properties away from the Hugoniot curve [46]. These attempts have been crucial in trying to understand how the properties of the Earth's liquid core deviate from those of pure liquid Fe. We present here a brief comparison with these experimentally based extrapolations for the two quantities that determine the seismic properties of the outer core: the density ρ and the adiabatic bulk modulus K_S.

Since the outer core is in a state of turbulent convection, the variation of its thermodynamic properties with depth is expected to follow an adiabat. We therefore present our comparisons on adiabats specified by their temperature T_ICB at $p = 330$ GPa, which is the pressure at the inner-core/outer-core boundary (ICB) [47]. We choose the two temperatures $T_\mathrm{ICB} = 5000$ and 7000 K, because the results of Sec. IV indicate that the melting temperature at the ICB pressure lies between these limits. Our comparisons (Tables IV and V) show that the uncorrected *ab initio* density is very close (within a few tenths of a percent) to the extrapolated experimental data at $p = 150$ GPa, and in slightly poorer agreement (within ~ 1.5 %) at $p = 350$ GPa. As expected, the free-energy correction lowers the predicted density, resulting in larger discrepancies with experiment of 1.5 % and 2.5 % at $p = 150$ and 350 GPa respectively. Our uncorrected *ab initio* K_S values also agree more closely with the experimental data, being typically within 2 %, while the corrected predictions disagree with the data by up to 8 %. However, given the closer agreement between *ab initio* and experiment on the Hugoniot (Sec. V), it is possible that some of the disagreements may be due to deficiencies in the experimental extrapolation.

VII. DISCUSSION AND CONCLUSIONS

In assessing the reliability of our results, we consider three sources of error: first, the uncontrolled DFT errors inherent in the GGA for exchange and correlation energy; second, the controllable errors in the detailed electronic-structure implementation of GGA, and specifically in the use of PAW to calculate the total *ab initio* (free) energy $U_\mathrm{AI}(\mathbf{R}_1, \ldots \mathbf{R}_N; T_\mathrm{el})$ for each set of atomic positions $\mathbf{R}_1, \ldots \mathbf{R}_N$; third, the statistical-mechanical errors, including system-size effects. We have endeavoured to reduce errors of the third kind below 10 meV/atom for the liquid. In our earlier free-energy calculations on the h.c.p. solid [11], the corresponding error was estimated as ~ 15 meV/atom. Taking these errors together, and recalling that the resulting error in melting temperature T_m is roughly the combined free-energy error divided by Boltzmann's constant, we find an expected T_m error of *ca.* ± 300 K. We have also attempted to control errors of the second kind by changing the division between core and valence states and by reducing the core radius. These tests suggest that the associated error in T_m is probably no more than *ca.* ± 100 K. The inherent DFT errors are more difficult to quantify, but we have demonstrated that the known discrepancies in the low-temperature $p(V)$ relation for h.c.p. Fe almost certainly lead to an overestimate of T_m by *ca.* 350 K at 50 GPa and *ca.* 70 K at 300 GPa, and we have corrected for this. We have also seen the significant shifts in the Hugoniot curves resulting from DFT errors. We believe the remaining uncertainty in T_m from this source could be as much as 300 K.

Our attempts to correct for DFT errors give a melting curve which is in quite good agreement with the recent measurements of Shen *et al.* [19], and with estimates based on shock data [23]; the methods used to estimate temperature in the shock experiments are also supported by our *ab initio* results for Grüneisen parameter γ and specific heat C_v [11]. Our melting curve is still above the experimental data of Boehler [17] by ~ 800 K in the pressure region up to *ca.* 100 GPa. We cannot rule out the possibility that some of this discrepancy is due to our DFT errors. Our substantial disagreement with the *ab initio* melting curve of Laio *et al.* [25] must be due to other reasons. We are currently working with authors of Ref. [25] to discover the cause of the disagreement, and we hope to report on this in the future.

A key part of our strategy for eliminating system-size errors in the calculated free energies is the use of an empirical reference model which accurately reproduces the fluctuations of total energy. At first sight, the use of a reference model based on a purely repulsive pair potential might seem surprising, since it does not explicitly include a description of metallic bonding. An empirical reference model (there called an 'optimised potential model') is also used in the work of Laio *et al.* [25], though they use it in a different way from us. Their optimised potential model is a form of the 'embedded atom model' (EAM) [48–50], which explicitly includes metallic bonding. As described in our earlier work [11], we have investigated the consequences of using the EAM as a reference model. We showed there that for present purposes fluctuations of the bonding energy are negligible, and that under these circumstances the EAM is almost exactly equivalent to a model based on repulsive pair potentials. We also showed that there is no numerical advantage in using the EAM as reference model for the calculation of free energies. The use of different reference models *per se* therefore appears to have nothing to do with the current disagreement between *ab initio* melting curves.

The agreement of our *ab initio* results with the limited data from shock experiments on the liquid is reasonably satisfactory. In particular, our predicted Hugoniot relation $p_{\rm H}(V_{\rm H})$ is almost as good as we found earlier for the solid. The adiabatic sound velocity of the liquid is also predicted to within $1-3$ %, the discrepancy depending on whether or not we attempt to correct for DFT errors. The good agreement for the Grüneisen parameter γ is also encouraging. Our results for the h.c.p. solid [11] indicated that γ varies little with pressure or temperature for $100 < p < 300$ GPa and $4000 < T < 6000$ K, and has a value of *ca.* 1.5. Our present results indicate that the same is true of the liquid.

The *ab initio* free-energy techniques outlined here could clearly be adapted to a wide range of other problems, so that melting curves could be calculated for many materials, including those of geological interest, like silicates. We have recently completed *ab initio* calculations of the melting curve of aluminium up to pressures of 150 GPa, which are in excellent agreement with static-compression and shock data, as will be reported elsewhere [51].

In conclusion, we have shown how *ab initio* free-energy calculations based on thermodynamic integration can be used to obtain the melting curve and the volume and entropy of melting of a material over a wide pressure range. We have emphasised that the key requirement on the reference system used in thermodynamic integration is that it faithfully mimics the fluctuations of *ab initio* energy in thermal equilibrium. Our *ab initio* melting curve of Fe over the pressure range $50-350$ GPa agrees fairly well with experimental data obtained from both static-compression and shock techniques, but significant discrepancies remain to be resolved. Our *ab initio* predictions for quantities obtained directly from shock experiments, including the Grüneisen parameter of the liquid, agree closely with the measured data in most cases.

[1] O. Sugino and R. Car, Phys. Rev. Lett. **74**, 1823 (1995).

[2] E. Smargiassi, P. A. Madden, Phys Rev B **51**, 117 (1995).

[3] G. A. de Wijs, G. Kresse and M. J. Gillan, Phys. Rev. B **57**, 8223 (1998).

[4] D. Alfè, G. A. de Wijs, G. Kresse and M. J. Gillan, Int. J. Quant. Chem., **77**, 871 (2000).

[5] B. B. Karki, R. M. Wentzcovitch, S. de Gironcoli, S. Baroni, Phys. Rev. B, **62**, 14750 (2000).

[6] A. I. Lichtenstein, R. O. Jones, S. de Gironcoli, S. Baroni, Phys. Rev. B **62**, 11487 (2000).

[7] J. J. Xie, S. P. Chen, J. S. Tse, S. de Gironcoli, S. Baroni, Phys. Rev. B, **60**, 9444 (1999).

[8] J. J. Xie, S. de Gironcoli, S. Baroni, M. Scheffler, Phys. Rev. B, **59**, 965 (1999).

[9] M. Lazzeri, S. de Gironcoli, Phys. Rev. Lett., **81**, 2096 (1998).

[10] P. Pavone, S. de Gironcoli, S. Baroni, Phys. Rev. B, **57**, 10421 (1998).

[11] D. Alfè, G. D. Price, M. J. Gillan, Phys. Rev. B, **64**, 045123 (2001).

[12] D. Alfè, M. J. Gillan and G. D. Price, Nature, **401**, 462 (1999).

[13] F. Birch, J. Geophys. Res., **69**, 4377 (1964).

[14] A. E. Ringwood, Geochem. J., **11**, 111 (1977).

[15] J.-P. Poirier, Phys. Earth Planet. Inter. **85**, 319 (1994).

[16] For a brief review of experiments on the melting curve of Fe, see e.g. O. L. Anderson and A. Duba, J. Geophys. Res. Sol. Earth, **102**, 22659 (1997).

[17] R. Boehler, Nature **363**, 534 (1993).

[18] S. K. Saxena, G. Shen, and P. Lazor, Science, **264**, 405 (1994).

[19] G. Shen, H. Mao, R. J. Hemley, T. S. Duffy and M. L. Rivers, Geophys. Res. Lett. **25**, 373 (1998).

[20] D. Errandonea, B. Schwager, R. Ditz, C. Gessmann, R. Boehler, M. Ross, Phys. Rev. B **63**, 132104 (2001).

[21] Q. Williams, R. Jeanloz, J. D. Bass, B. Svendesen, T. J. Ahrens, Science **286**, 181 (1987).

[22] C. S. Yoo, N. C. Holmes, M. Ross, D. J. Webb and C. Pike, Phys. Rev. Lett. **70**, 3931 (1993).

[23] J. M. Brown and R. G. McQueen, J. Geophys. Res. **91**, 7485 (1986).

[24] J. H. Nguyen and N. C. Holmes, unpublished.

[25] A. Laio, S. Bernard, G. L. Chiarotti, S. Scandolo and E. Tosatti, Science **287**, 1027 (2000).

[26] A. B. Belonoshko, R. Ahuja, and B. Johansson, Phys. Rev. Lett. **84**, 3638 (2000).

[27] D. Frenkel and B. Smit, *Understanding Molecular Simulation*, Academic Press, San Diego (1996).

[28] Y. Wang and J. Perdew, Phys. Rev. B **44**, 13298 (1991).

[29] J. P. Perdew, J. A. Chevary, S. H. Vosko, K. A. Jackson, M. R. Pederson, D. J. Singh and C. Fiolhais, Phys. Rev. B **46**, 6671 (1992).

[30] L. Stixrude, R. E. Cohen and D. J. Singh, Phys. Rev. B **50**, 6442 (1994).

[31] P. Söderlind, J. A. Moriarty and J. M. Willis, Phys. Rev. B **53**, 14063 (1996).

[32] L. Vočadlo, G. A. de Wijs, G. Kresse, M. J. Gillan and G. D. Price, Faraday Disc. **106**, 205 (1997).

[33] D. Alfè, G. Kresse and M. J. Gillan, Phys. Rev. B, **61**, 132 (2000).

[34] P. E. Blöchl, Phys. Rev. B **50**, 17953 (1994).

[35] G. Kresse and D. Joubert, Phys. Rev. B **59**, 1758 (1999).

[36] S. H. Wei and H. Krakauer, Phys. Rev. Lett., **55**, 1200 (1985).

[37] D. Vanderbilt, Phys. Rev. B **41**, 7892 (1990).

[38] G. Kresse and J. Furthmüller, Phys. Rev. B **54**, 11169 (1996).

[39] G. Kresse and J. Furthmüller, Comput. Mater. Sci. **6**, 15 (1996).

[40] D. Alfè, Comp. Phys. Commun., **118**, 31 (1999).

[41] N. D. Mermin, Phys. Rev. **137**, A1441 (1965).

[42] B. B. Laird and A. D. J. Haymet, Mol. Phys., **75**, 71 (1992).

[43] K. Johnson, J. A. Zollweg, and E. Gubbins, Mol. Phy. **78**, 591 (1993).

[44] H. J. Monkhorst and J. D. Pack, Phys. Rev. B **13**, 5188 (1976).

[45] J.-P. Poirier, *Introduction to the Physics of the Earth's Interior*, Cambridge University Press, Cambridge (1991), ch. 4.

[46] W. W. Anderson and A. T. J. Ahrens, J. Geophys. Res. **99**, 4273 (1994).

[47] A. M. Dziewonski and D. L. Anderson, Phys. Earth Planet. Inter. **25**, 297 (1981).

[48] M. S. Daw, S. M. Foiles, and M. I. Baskes, Mat. Sci. Rep., **9**, 251 (1993).

[49] M. I. Baskes, Phys. Rev. B, **46**, 2727 (1992).

[50] A. B. Belonoshko, and R. Ahuja, Phys. Earth Planet. Inter., **102**, 171 (1997).

[51] L. Vočadlo and D. Alfè, unpublished.

T (K)	ρ (kg m^{-3})				
	9540	10700	11010	12130	13300
3000	0.097 (60)				
4300		0.085 (132)			
5000		0.089 (140)			
6000	0.104 (90)	0.096 (151)	0.089 (170)	0.103 (251)	0.125 (360)
7000		0.093 (161)	0.098 (181)	0.109 (264)	0.131 (375)
8000		0.092 (172)	0.099 (191)	0.104 (275)	0.124 (390)

TABLE I. Normalised fluctuation strength σ (see text) characterising the accuracy with which the inverse-power reference model mimics the energy fluctuations of *ab initio* liquid Fe. Values of σ (eV units) are given for a set of AIMD simulations at different densities ρ and temperatures T. Pressure at each thermodynamic state (GPa units) is given in parenthesis.

	$(\delta U_{\rm th}(N) - \delta U_{\rm th}(241))/N$ (eV)	$(\delta U_{\rm th}(4k) - \delta U_{\rm th}(\Gamma))/N$ (eV)	σ (eV)
67	-0.009 ± 0.002	0.009 ±0.003	0.085
89	-0.012 ± 0.001	0.007 ±0.002	0.073
107	-0.010 ± 0.001	0.006 ±0.002	0.083
127	0.004 ± 0.001	0.000 ±0.002	0.086
157	0.001 ± 0.001	0.001 ±0.002	0.069
199	0.001 ± 0.001		0.082
241	0.000 ± 0.001	0.001 ±0.002	0.101

TABLE II. Dependence on number of atoms N in the simulation cell of size errors and k-point sampling errors in the quantity $\delta U_{\rm th}$ entering the *ab initio* free energy of liquid Fe (see Eqn (15)). Second column reports $\delta U_{\rm th}/N$ (eV units) with a constant offset chosen so that the reported value for the largest system size is zero. Third column reports difference of $\delta U_{\rm th}/N$ between simulations using four k-points and Γ-point sampling. Fourth column reports normalised fluctuation strength σ (see text) for different system sizes.

T (K)	$N^{-1} \int_0^1 d\lambda \langle \Delta U \rangle_\lambda$ (eV)	$\langle (\delta \Delta U)^2 \rangle_{\rm AI}/2N k_{\rm B} T$ (eV)
4300	0.012	0.012
6000	0.010	0.009
8000	0.006 (0.010)	0.006 (0.010)

TABLE III. Difference $F_{\rm AI} - F_{\rm ref}$ between free energies of *ab initio* and reference systems calculated in two ways: by full thermodynamic integration (column 2) as in Eqn (4), and by the second-order fluctuation approximation (column 3) as in Eqn (6). Free energy differences are given per atom in eV units for three temperatures at the density $\rho = 10700$ kg m^{-3}. Values in parenthesis refer to the density $\rho = 13300$ kg m^{-3}.

P (GPa)	ρ (kg m⁻³) This work T = 5000 K	T = 7000 K	Experiments T = 5000 K	T = 7000 K
150	11075 (10930)	10806 (10659)	11110	10800
200	11738 (11625)	11477 (11350)	11870	11560
250	12323 (12220)	12059 (11950)	12440	12180
300	12844 (12756)	12575 (12481)	13000	12800
350	13315 (13232)	13043 (12970)	13550	13290

TABLE IV. Comparison of *ab initio* and experimental density ρ of liquid Fe on two adiabats, with adiabats specified by the temperature T at the pressure $p = 300$ GPa. *Ab initio* ρ values are given both without and with (in parenthesis) free-energy correction δF (see text).

P (GPa)	K_S (GPa) This work T = 5000 K	T = 7000 K	Experiments T = 5000 K	T = 7000 K
150	708 (662)	656 (613)	695	668
200	878 (838)	820 (781)	877	849
250	1050 (1010)	981 (944)	1058	1016
300	1220 (1180)	1140 (1103)	1232	1193
350	1384 (1350)	1296 (1264)	1400	1355

TABLE V. Comparison of *ab initio* and experimental adiabatic bulk modulus K_S of liquid Fe on two adiabats, with adiabats specified by the temperature T at the pressure $p = 330$ GPa. *Ab initio* K_S values are given both without and with (in parenthesis) free-energy correction δF (see text).
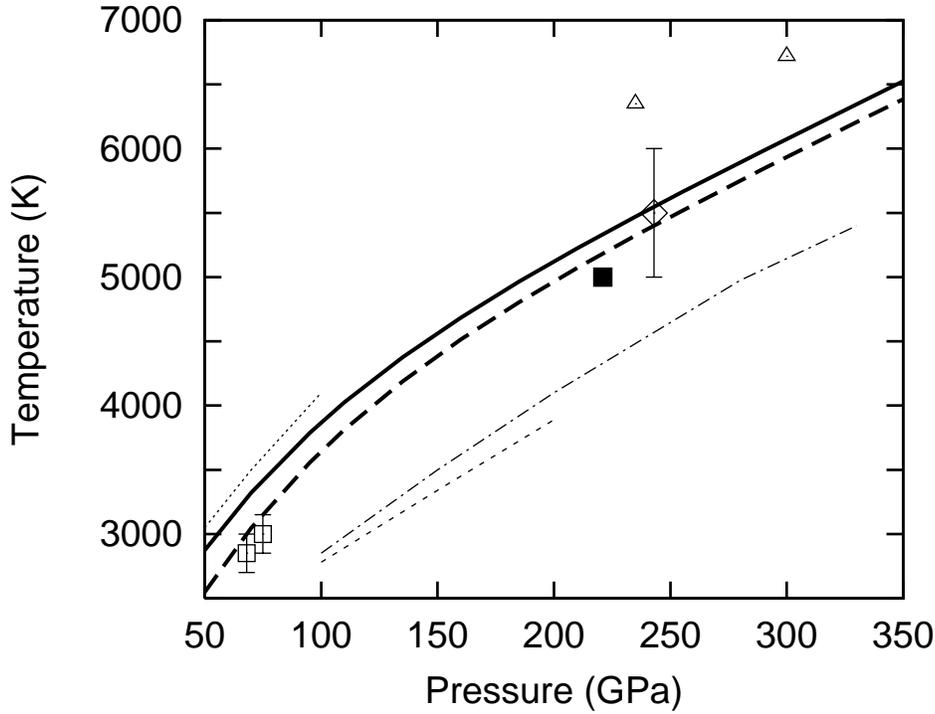
FIG. 1. Comparison of melting curve of Fe from present calculations with previous experimental and *ab initio* results: heavy solid and dashed curves: present work without and with free-energy correction (see text); chain curve: *ab initio* results of Ref. [25]; dots, light dashes and squares: DAC measurements of Refs. [21], [17] and [19]; triangles, diamond and solid square: shock experiments of Refs. [22], [23] and [24]. Error bars are those quoted in original references.
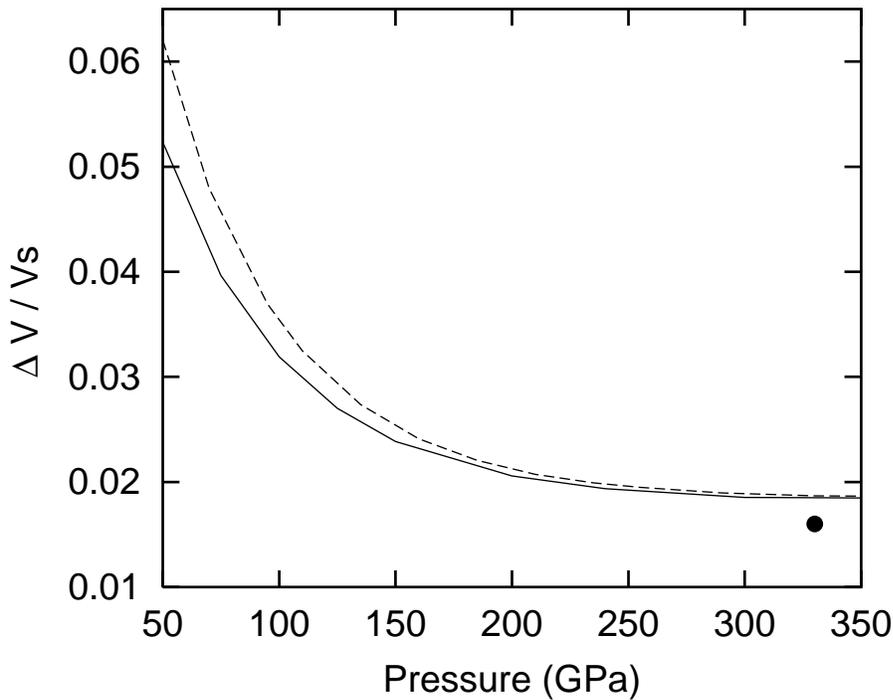

FIG. 2. *Ab initio* fractional volume change on melting of Fe as a function of pressure. Solid and dashed curves: present work, without and with free-energy correction (see text); black dot: Ref. [25].
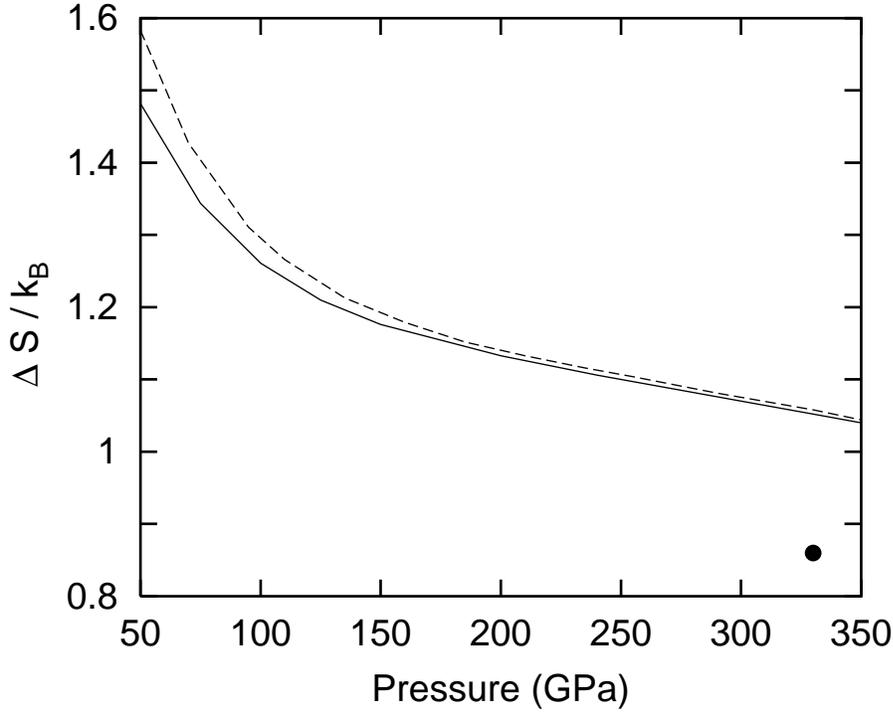
14

FIG. 3. *Ab initio* entropy change on melting per atom (units of Boltzmann's constant k_{B}). Solid and dashed curves: present work, without and with free-energy correction (see text); black dot: Ref. [25].
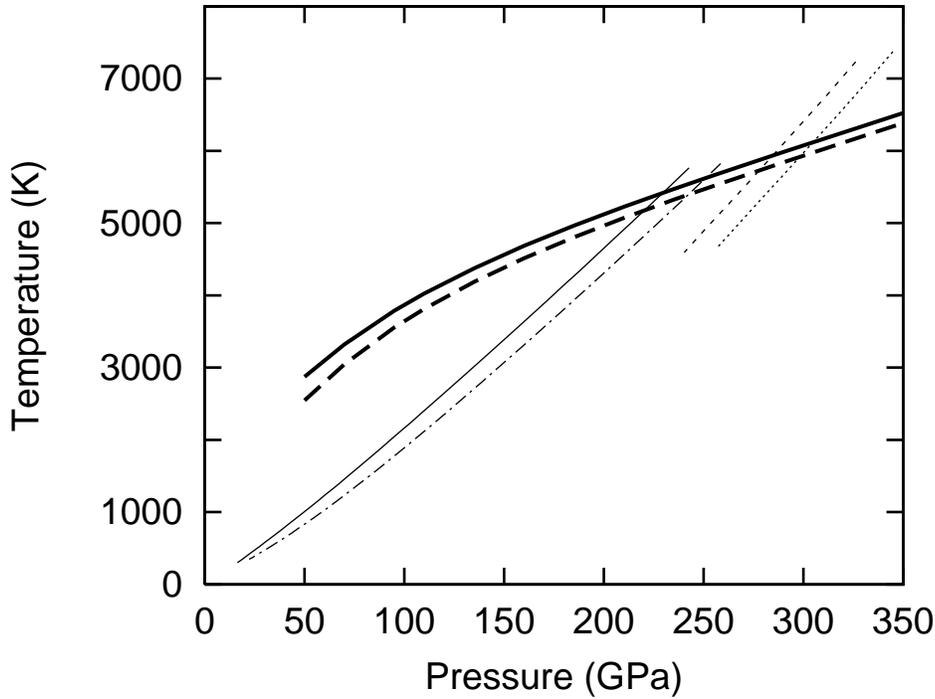

FIG. 4. Relation between *ab initio* melting curve and *ab initio* Hugoniot temperature-pressure curves. Heavy continuous and dashed curves: melting curves calculated without and with free-energy correction (see text); light continuous and chain curves: Hugoniot of solid without and with free-energy correction; light dashed and dotted curves: Hugoniot of liquid without and with free-energy correction.
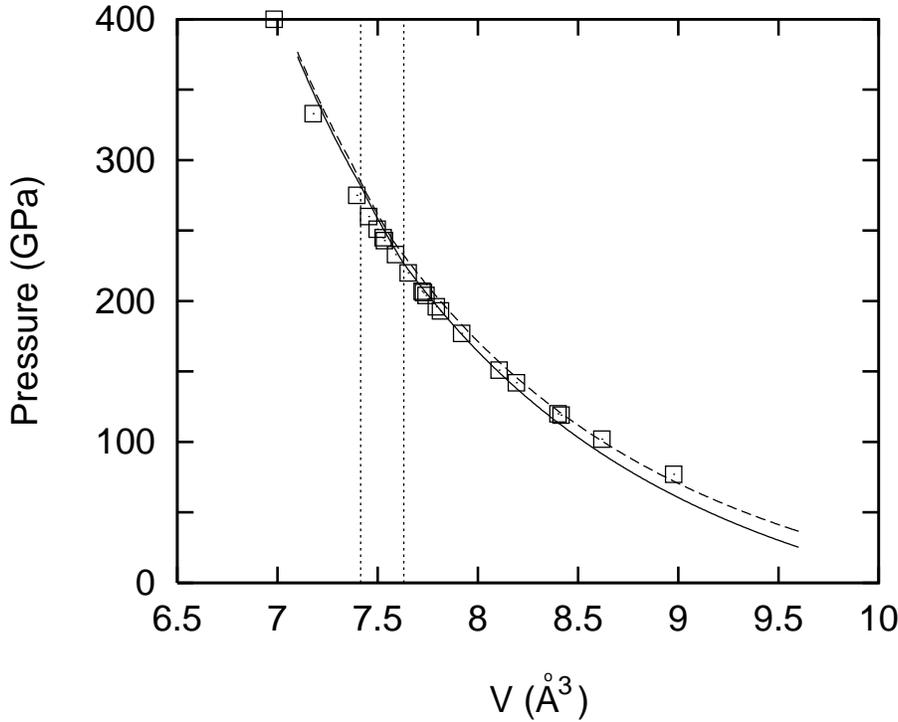
FIG. 5. *Ab initio* Hugoniot pressure-volume curve compared with experimental results of Ref. [23]. Solid and dashed curves: *ab initio* results without and with free-energy correction (see text); squares: experimental results. Vertical dotted lines indicate volumes at which melting starts and finishes according to present (uncorrected) *ab initio* results. To the right of rightmost vertical dotted line, curves represent solid Hugoniot from Ref. [11]; to the left of leftmost vertical line, curves represent present liquid Hugoniot.
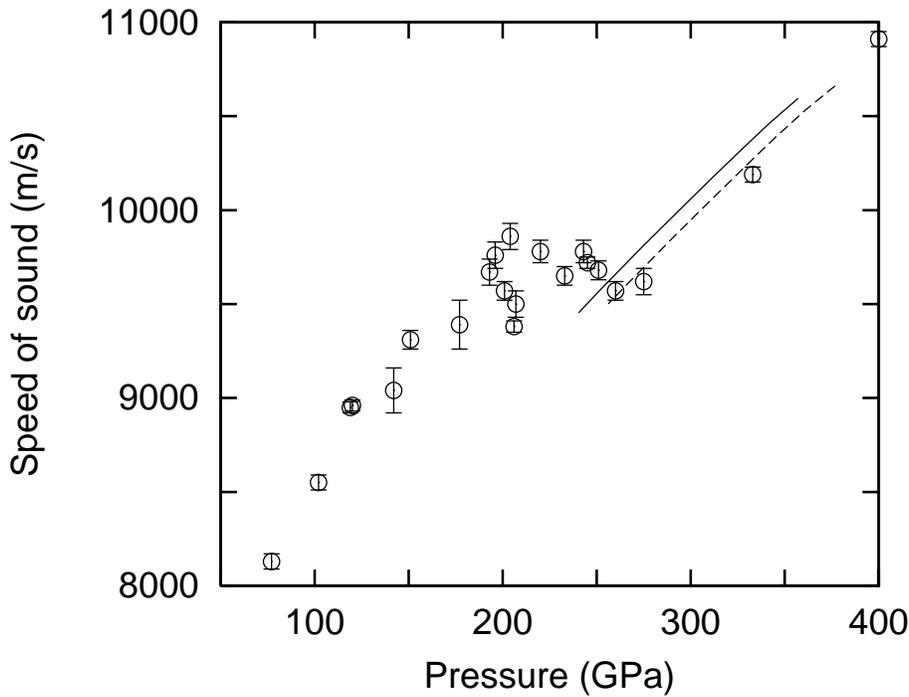

FIG. 6. Longitudinal speed of sound on the Hugoniot. Circles: experimental values from Ref. [23]; continuous and dashed curves: present *ab initio* values without and with free-energy correction (see text).